Palmitate-TLR4 Signaling Regulates the Histone Demethylase, JMJD3, in Macrophages and Impairs Diabetic Wound Healing

Authors

Frank M. Davis, M.D.[1]; Aaron denDekker, Ph.D.[1]; Amrita D. Joshi, Ph.D.[1]; Sonya J. Wolf, Ph.D.[1]; Christopher Audu, M.D., Ph.D.[1]; William J. Melvin, M.D.[1];

Kevin Mangum, M.D., Ph.D.[1]; Mary O'Riordan, Ph.D.[2] Steven L. Kunkel, Ph.D. [3]; Katherine A. Gallagher, M.D. [1,2]

Affiliations

[1]Section of Vascular Surgery, Department of Surgery, University of Michigan, Ann Arbor, MI.

[2]Department of Microbiology and Immunology, University of Michigan, Ann Arbor, MI.

[3]Department of Pathology, University of Michigan, Ann Arbor, MI.

Address for Correspondence:

Dr. Katherine A. Gallagher

University of Michigan Section of Vascular Surgery, Department of Surgery

Department of Immunology

This is the author manuscript accepted for publication and has undergone full peer review but has not been through the copyediting, typesetting, pagination and proofreading process, which may lead to differences between this version and the Version of Record. Please cite this article as doi: 10.1002/eji.202048651.

5364 Cardiovascular Center

1500 E. Medical Center Drive

Ann Arbor, MI 48109-5867

Telephone: (734) 936-5820

E-mail: kgallag@med.umich.edu

Keywords: Diabetes, macrophage, toll-like receptor, epigenetics, wound

Abbreviations

BSA	Bovine serum albumin
ChIP	Chromatin immunoprecipitation
DIO	Diet induced obesity
FA	Fatty acid
H3K27	Histone 3 lysine 27
H3K27me3	Histone 3 lysine 27 trimethylation
Jmjd3	Jumonji Domain Containing 3
IL	Interleukin
Mφ	Macrophage
MACs	Magnetic-activated cell sorting
MCP-1	Monocyte chemoattractant protein 1
MyD88	Myeloid differentiation primary response 88
NFκB	Nuclear factor kappa-light-chain-enhancer of activated B cells
T2D	Type 2 diabetes
TLR4	Toll-like receptor 4
TNF	Tumor necrosis factor alpha

SFA saturated fatty acid

Abstract

Chronic macrophage inflammation is a hallmark of type 2 diabetes (T2D) and linked to the development of secondary diabetic complications. T2D is characterized by excess concentrations of saturated fatty acids (SFA) that activate innate immune inflammatory responses, however mechanism(s) by which SFAs control inflammation is unknown. Using monocyte-macrophages isolated from human blood and murine models, we demonstrate that palmitate (C16:0), the most abundant circulating SFA in T2D, increases expression of the histone demethylase, Jmjd3. Upregulation of Jmjd3 results in removal of the repressive histone methylation (H3K27me3) mark on NFκB-mediated inflammatory gene promoters driving macrophage-mediated inflammation. We identify that the effects of palmitate are fatty acid specific, as laurate (C12:0) does not regulate Jmjd3 and the associated inflammatory profile. Further, palmitate-induced Jmjd3 expression is controlled via TLR4/MyD88-dependent signaling mechanism, where genetic depletion of TLR4 (*Tlr4*$^{-/-}$) or MyD88 (*MyD88*$^{-/-}$) negated the palmitate-induced changes in Jmjd3 and downstream NFκB-induced inflammation. Pharmacological inhibition of Jmjd3 using a small molecule inhibitor (GSK-J4) reduced macrophage inflammation and improved diabetic wound healing. Together, we conclude that palmitate contributes to the chronic Jmjd3-mediated activation of macrophages in diabetic peripheral tissue and a histone demethylase inhibitor-based therapy may represent a novel treatment for non-healing diabetic wounds.

INTRODUCTION

Obesity has become a global epidemic and is associated with an increased risk of development of chronic inflammatory diseases, including insulin resistance and type 2 diabetes (T2D)[1]. Within T2D, dysregulated macrophage-mediated inflammation represents a hallmark of disease progression. Macrophages have diverse functions in tissues depending on the local environment and other systemic factors. Typically, macrophages in tissues exist along a spectrum where M1 "classically activated" macrophages contribute to tissue inflammation and bactericidal activity, and M2 "alternatively activated" macrophages promote reduction of inflammation, growth factor secretion, and tissue repair[2]–[4]. It has been demonstrated that during development of obesity and T2D, macrophages undergo a ''phenotypic switch'' from an anti-inflammatory phenotype to a proinflammatory state and this conversion has been linked to the emergence of systemic insulin resistance[5]. Further, this chronic diabetic macrophage inflammation can impact secondary complications of diabetes including diabetic wound healing. During normal response to injury, monocytes are recruited from the blood and home to injured tissues where they become macrophages that initially exhibit a pro-inflammatory phenotype with increased production of inflammatory cytokines and enhanced pathogen killing capacity. As tissue repair progresses, these

macrophages convert to a predominantly anti-inflammatory phenotype to promote resolution. This macrophage plasticity in tissues allows for normal repair to occur. However, in T2D the pro-inflammatory to anti-inflammatory macrophage phenotypic switch is impaired and inflammatory macrophages accumulate in tissues with associated increased expression of IL12, TNF-α, IL1β, MCP-1 and other inflammatory cytokines[6],[7]. The etiology of this chronic diabetic macrophage-mediated inflammation is presently unknown but is likely multifactorial.

Epigenetic regulation of gene expression plays a major role in the phenotype and function of immune cells in both normal and pathologic conditions by controlling downstream gene expression patterns (9). We and others have shown that histone methylation regulates immune-mediator expression in macrophages both *in vitro* and *in vivo* (10, 11). Jmjd3 is a histone demethylase with site specificity for histone 3 lysine 27 (H3K27). H3K27 trimethylation (H3K27me3) of gene promoter regions is associated with a condensed chromatin conformation and thus genes are effectively silenced. Upregulation of Jmjd3 results in removal of the inhibitory histone methylation and activates gene transcription. Although the role of Jmjd3 in oncogenesis has been investigated, few studies have examined the role of Jmjd3 in innate immunity or in T2D [11]. We have recently identified that Jmjd3 may control inflammation in bone marrow progenitor cells in T2D, however the mechanisms that control Jmjd3 activation and its downstream activity in T2D peripheral macrophages remain unknown.

In patients with T2D, plasma and tissue levels of fatty acids (FA) are elevated. Recent studies indicate a specific proinflammatory effect of saturated fatty acids (SFA) on several cell types[12],[13]. For example, in murine macrophages, SFA, but not unsaturated FA, induced expression of IL-1β and iNOS (14). Palmitate (C16:0) is the most abundant SFA in plasma, and together with stearate (C18:0), it constitutes 90% of circulating SFA [13]. SFAs can activate inflammatory signaling pathways through various mechanisms, including the innate immune receptor TLR4 [14]–[16]. TLR4 is a member of the family of pattern recognition receptors that play a key role in innate immune cell function by activating downstream proinflammatory pathways in response to microbial pathogens (e.g., LPS) and damaged tissue-associated signals (DAMPs).

Given the importance of TLR4 on immune cell function, particularly macrophage function, as well as the known increase in the SFA palmitate in T2D, we investigated the role of palmitate stimulation of the TLR4 receptor in the regulation of Jmjd3-mediated chronic inflammation in macrophages. Here, we demonstrate that the SFA palmitate (C16:0) drives chronic macrophage mediated inflammation via upregulation of the histone demethylase, Jmjd3. Specifically, using primary macrophages isolated from human patients and murine models, we show that palmitate stimulation increases expression of the histone demethylase, Jmjd3, which upregulates inflammatory cytokine levels by removal of the repressive H3K27me3 mark on NFkB-regulated gene promoters. Further, genetic depletion of TLR4

(*Tlr4*$^{-/-}$) or MyD88 (*MyD8*$^{-/-}$) negated this palmitate inflammatory stimulation in macrophages, suggesting palmitate-induced inflammation is dependent on the TLR4/MyD88 pathway. Lastly, mice treated with a Jmjd3 specific inhibitor (GSK-J4) had reduced macrophage inflammation and improved wound healing in a diabetic murine model. These findings provide new mechanistic insight linking palmitate-TLR4 stimulation and Jmjd3-mediated to the chronic macrophage inflammation in T2D.

RESULTS

Palmitate epigenetically regulates macrophage-mediated inflammatory cytokines via Jmjd3 mechanism

Increasing evidence suggests that proper wound healing requires the establishment of a regulated inflammatory response mediated by macrophages [6],[17],[18]. Since Jmjd3 is important for NFκB-mediated inflammation in macrophages[19],[20]; we examined if palmitate, a known SFA that is increased in diabetes, stimulation altered Jmjd3 expression *in vitro* in macrophages. To study this, BMDMs from C57BL/6 mice were stimulated with BSA, laurate (50 uM), palmitate (200 uM) or LPS (10 ng/ml) for 6 hours and analyzed by for *Jmjd3* gene expression. The dosing of laurate and palmitate were specifically chosen to approximate known plasma concentrations in T2D patients [21],[22]. We found that palmitate significantly increased *Jmjd3*, even to a greater degree than LPS stimulation (Figure 1A). This effect on *Jmjd3* expression was not seen with stimulation from other SFAs such as laurate (C12:0). Next, to identify if palmitate can increase NFκB-mediated inflammatory cytokines important in wound repair, we examined BMDMs stimulated with BSA, laurate (50 uM), palmitate (200 uM) or LPS (10 ng/ml) and analyzed by for *Il1b* and *Il12* gene expression, two key inflammatory cytokines elevated in diabetes that are known to play a critical role in wound repair. We found significant increases in *Il1b* and *Il12* inflammatory genes following palmitate stimulation (Figure 1B). Further, to determine if increased Jmjd3 epigenetically regulates these NFκB-mediated inflammatory genes important in wound healing we examined the NFκB binding sites on the gene promoters of *Il1b* and *Il12* for H3K27me3, the methylation mark regulated by Jmjd3, following palmitate or laurate stimulation. We found that palmitate stimulation decreased H3K27me3 (an inhibitory mark) on the promoter(s) of these genes, resulting in the corresponding increased gene expression (Figure 1B). This reduction of H3K27me3 on inflammatory gene promoters was not seen when BMDMs were stimulated with BSA or laurate (50 uM). These data may indicate that NFκB-mediated inflammatory gene transcription in macrophages is controlled, at least partially, by Jmjd3.

Prior research has demonstrated that external stimuli, including LPS, can drive *Jmjd3* expression[23]. One important receptor vital for activation of inflammatory signaling pathways is the TLR4 receptor. Given that both LPS and palmitate were shown to increase

Jmjd3 expression we examined the role of TLR4/MyD88 in the palmitate-mediated regulation of *Jmjd3*. BMDMs were isolated from *Tlr4*$^{-/-}$ and *MyD88*$^{-/-}$ on a C57BL/6 background. Following stimulation with palmitate (200 uM) or laurate (50 uM) we found a significant increase in *Jmjd3* expression following palmitate stimulation in control BMDMs, but this Jmjd3 elevation was absent in TLR4 and MyD88-deficient BMDMs. Further TLR4 and MyD88-deficient BMDMs, displayed reduced levels of NFκB-mediated inflammatory cytokines, *Il1b* and *Il12* in response to palmitate (Figure 1C). Taken together, these results indicate that palmitate-induced Jmjd3, regulates NFκB-mediated inflammatory genes important in wound healing, via an H3K27me3-mediated mechanism and that Jmjd3 may be controlled, in part, by a TLR4-MyD88 mediated pathway.

Palmitate controls Jmjd3-mediated inflammatory cytokines in wound macrophages.

In order to examine the role of palmitate induced Jmjd3 on *in vivo* wound macrophage phenotype, C57Bl/6 mice were subjected to 6 mm full-thickness wounds as previously described [17], and macrophages ($CD11b^+[CD3^-CD19^-NK1.1^-Ly6G^-]$) were isolated from wounds via magnetic-activated cell sorting (MACs) on day 3 and 5 post-wounding. Wound macrophages were treated *ex vivo* with palmitate (200 uM) or laurate (50 uM) for 24 hours. We first examined *Jmjd3* gene expression and found it was significantly increased in wound macrophages following palmitate stimulation (Figure 2A). In order to determine whether changes in Jmjd3 in wound macrophages corresponded to changes in the NFκB-mediated inflammatory cytokines, we examined *ex vivo* wound macrophages at multiple days post injury for *Il1b* and *Il12*. We found significantly increased *Il1b* and *Il12* gene expression and protein production associated with palmitate stimulation as compared to laurate or BSA (Figure 2B, C and Supplemental Figure 1A-D). To determine if increased Jmjd3 epigenetically regulates IL1β and IL12 *in vivo* wound macrophages, we isolated wound macrophages ($CD11b^+[CD3^-CD19^-NK1.1^-Ly6G^-]$) on day 3 via MACs sorting and examined the NFκB binding sites on the gene promoters of *Il1b* and *Il12* for H3K27me3, following palmitate, laurate or BSA stimulation. We found that palmitate stimulation decreased H3K27me3 on the NFκB binding site of the promoter(s) of these genes, likely resulting in the corresponding increased gene expression in wound macrophages (Figure 2B, C). To further investigate the relationship between palmitate stimulation and Jmjd3-mediated inflammatory cytokine production, we isolated wound macrophages ($CD11b^+[CD3^-CD19^-NK1.1^-Ly6G^-]$) on day 3 via MACs sorting and stimulated the macrophages with palmitate with or without co-administration of a Jmjd3 specific inhibitor (GSK-J4, 5μM). Palmitate stimulation resulted in marked upregulation of inflammatory cytokine expression (*Il1b* and *Il12*), although not as significant an influence as the positive control LPS. However, the palmitate mediated inflammatory cytokine upregulation was negated with Jmjd3 inhibition (GSK-J4) (Figure 2D). This data may indicate that NFκB-mediated inflammatory gene transcription *in vivo* wound macrophages is controlled, at least partially, by the histone demethylase, Jmjd3.

Palmitate regulates JMJD3-mediated inflammation in human monocytes.

In order to evaluate if our findings may be translatable to human patients, we isolated blood monocytes (CD14+) from peripheral blood of healthy controls. Human monocytes were stimulated with BSA, laurate (50 uM), palmitate (200 uM) or LPS (10 ng/ml) for 12 hours. *JMJD3* expression was examined and found to be significantly increased following palmitate stimulation (Figure 3A). This increased *JMJD3* expression was not seen following laurate stimulation. We next examined whether stimulation with palmitate can increase NFκB-mediated inflammatory cytokines. We found that *TNFα* and *IL1* are increased in human monocytes following stimulation with palmitate compared to controls (Figure 3B). These findings may partially explain the chronic inflammatory state of non-healing T2D wounds, where palmitate levels are significantly increased, as are the NFκB-mediated inflammatory cytokines, *TNFα* and *IL1β*.

Diabetic murine wounds treated with a Jmjd3 small molecule inhibitor demonstrate improved healing

Since palmitate appeared to regulate Jmjd3 *in vitro* and *in vivo* murine wound macrophages and in human monocytes, we examined if specific blockade of Jmjd3 in diabetic murine wounds improved healing, possibly by altering wound macrophage phenotype. Given that prior publications have demonstrated that genetic knockout of Jmjd3 results in mid-gestation lethality in mice secondary to developmental abnormalities [24], we pursued a pharmacological based approach. Specifically, six millimeter punch biopsy wounds were generated in DIO mice and the Jmjd3 inhibitor (GSK-J4) (10 mg/kg) was administered 3 days prior to wounding and daily immediately following wounding. This was done in order to assure that the drug was at adequate levels prior to wounding. Wounds were then analyzed daily for 7 days. Diabetic mice treated with GSK-J4 demonstrated improved wound healing compared to control treated animals (Figure 4A). To determine if Jmjd3 inhibition regulates macrophage inflammatory cytokine production, circulating monocytes and wound macrophages were isolated from DIO mice with or without GSK-J4 administration via MACs sorting. We found that DIO mice that received the Jmjd3 inhibitor (GSK-J4) had a significant reduction in inflammatory cytokine expression in both circulating monocytes and wound macrophages, but no difference in granulation tissue deposition likely resulting from minimal impact of Jmjd3 inhibition on fibroblast deposition (Figure 4B, C and Supplemental Figure 2).These results suggest that Jmjd3 inhibition may improve diabetic wound repair, possibly by regulating macrophage-mediated inflammation.

DISCUSSION

Macrophages are involved in the initiation and resolution of inflammatory processes, and their dysregulation contributes to chronic inflammatory diseases [25]. In the case of diabetes and metabolic syndromes, the production of proinflammatory cytokines by macrophages correlates with the serum concentration of SFA whereby increased SFA levels modify peripheral macrophage effector functions [26],[27]. However, the mechanisms of how SFAs regulate the macrophage inflammatory state is unclear [17],[28]–[31]. Herein, we identify the SFA palmitate (C16:0), which is highly upregulated in diabetes, drives chronic macrophage mediated inflammation via the epigenetic enzyme Jmjd3. Specifically, using primary macrophages isolated from human patients and our murine model, we show that palmitate stimulation increases expression of the histone demethylase, Jmjd3, which upregulates NFkB-mediated inflammatory cytokine levels by removal of the repressive histone 3 lysine 27 trimethylation (H3K27me3) mark on gene promoters. Further, genetic depletion of TLR4 (*Tlr4*$^{-/-}$) or MyD88 (*MyD88*$^{-/-}$) negated this palmitate inflammatory stimulation suggesting palmitate inflammation is dependent on the TLR4/MyD88 pathway. Lastly, mice treated with a Jmjd3 specific inhibitor (GSK-J4) had decreased macrophage imflammatory cytokine production and improved rates of diabetic wound healing. Taken together, our findings suggest that palmitate-TLR4 signaling regulates Jmjd3-mediated inflammation in diabetic myeloid cells and leads to impaired diabetic wound healing (Figure 5). These findings define potential therapeutic targets to correct impairments in the inflammatory program in diabetic wound macrophages that contribute to dysregulated healing.

Substantial progress has been made in understanding the ability of fatty acids to activate TLR4 signaling through *in vitro* and *in vivo* studies[14]–[16],[32],[33]. Initial studies hypothesized that SFAs were direct ligands to TLR4[34]. In general support of this idea, the principal component of LPS responsible for its immunostimulatory activity is the lipid A region, which contains numerous saturated fatty acyl chains that are required for binding to and activating TLR4. Importantly, consistent with this previous work, we observed a protective effect of TLR4 deficiency on SFA induced macrophage activation in two independent loss-of-function models, *Tlr4*$^{-/-}$ mice and *MyD88*$^{-/-}$ mice[35]. Despite progress of these previous studies, the precise downstream mechanism by which the TLR4 pathway contributes to chronic macrophage inflammation remains unknown. Most complex diseases, including obesity and diabetes, are result of genetic and environmental interactions. One of the mechanisms underlying the ability of environmental factors, such as diet, to affect gene expression, involves their capacity to reprogram the epigenome[36],[37]. Indeed, dietary fatty acids have been shown to differentially regulate histone methylation in renal[38] and retinal epithelial cells[39] resulting in aberrant gene expression and cellular dysfunction. Recently, we and others have shown that histone methylation also regulates immune-

mediator expression in *in vitro* and *in vivo* macrophages[9],[10]. Specifically, the histone demethylase, Jmjd3, was found to be upregulated in diabetic macrophages contributing to chronic inflammation[9]. Here we found that palmitate induced *Jmjd3* expression resulting in removal of the inhibitory histone methylation mark (H3K27me3) on the promoters of inflammatory cytokines. Our findings provide a mechanistic basis for how diabetes results in a macrophage phenotypic switch to a more proinflammatory 'M1' phenotype, leading to increased inflammation and eventually the development of obesity-associated metabolic diseases. Further, the current findings support the theory that the diabetic milieu and elevated SFAs alter immune cell phenotypes via an epigenetic based mechanisms[40],[41]. These epigenetic changes can contribute to a phenomenon known as 'metabolic memory' where chromatin modifications persist even after a normal physiological environment is restored[41].

Given the importance of Jmjd3, particularly in relation to the regulation of macrophage phenotype in response to fatty acids, we investigated if inhibition of Jmjd3 alters diabetic macrophage function and improves wound healing. We demonstrate that administration of a Jmjd3 specific inhibitor, GSK-J4, led to improved early diabetic wound healing. This is in agreement with a recent study where treatment of macrophages with a selective Jmjd3 inhibitor led to alterations in proinflammatory cytokine levels[2]. Because macrophages exhibit different functional phenotypes as tissue repair progresses[42], the ability to modulate macrophage phenotype at a particular time after injury is an attractive therapeutic strategy. For example, a Jmjd3 antagonist may augment early macrophage-mediated inflammation and help the wound healing cascade to occur in a programmed fashion. Jmjd3 inhibitors are attractive for use in wounds because they can be locally administered, negating many of the toxic effects of systemic administration. The therapeutic potential of GSK-J4 has been previously demonstrated in human neuroblastoma cell lines in which Jmjd3 inhibition prevented aberrant cell growth and inflammatory endoplasmic reticulum stress[43].

Although this study produces insight into the mechanism(s) behind diabetic myeloid-mediated inflammation, some limitations must be addressed. While our study provides evidence that the SFA palmitate induces Jmjd3-mediated epigenetic modifications in macrophages driving inflammatory cytokine production, it is unlikely that the chronic inflammation exhibited in diabetes is solely due to palmitate. Indeed, TLR4 can also detect endogenous danger signals, DAMPs, that are released by stress or injured tissues. As such several reports have demonstrated that DAMPs interact with TLR4 and induce the production of inflammatory cytokines [44],[45]. At this time, it remains unknown if DAMP-mediated activation of the TLR4 pathway upregulates macrophage epigenetic modification, but further investigations are likely warranted. Additionally, although H3K27 trimethylation suggests a potential mechanism for palmitate-TLR4 mediated inflammation in diabetic macrophages, we acknowledge that other epigenetic modifications may play a role. Indeed, a recent study suggested that DNA methylation via DNMT1 may induce proinflammatory macrophage

activation in diabetes[46]. Thus, further studies assessing the role of palmitate in the regulation of other specific epigenetic enzymes and macrophage-mediated inflammation are relevant.

In summary, our findings indicate that palmitate induces TLR4/MyD88-dependent upregulation of Jmjd3 in human and murine macrophages. Further, Jmjd3-dependent epigenetic modifications in macrophages primed these macrophages towards a proinflammatory state with removal of the inhibitory histone methylation mark on inflammatory cytokines promoters. These findings suggest that Jmjd3 plays a significant role in dictating wound macrophage phenotype; furthermore, it may have significant relevance to macrophage-driven inflammation in other secondary complications of diabetes (44–46). Thus, pharmacological inhibition of Jmjd3 may be a reasonable therapeutic strategy for regulating the inflammatory response in diabetic repair.

MATERIALS AND METHODS

Mice

Mice were maintained in the University of Michigan pathogen-free animal facility, and all protocols were approved by and in accordance with the guidelines established by the Institutional Animal Care and Use Committee (UCUCA). Male C57BL/6, *Tlr4*$^{-/-}$, and *MyD88*$^{-/-}$ mice purchased from The Jackson Laboratory (Bar Harbor, ME) were maintained on a normal chow diet (13.5% kcal fat; LabDiet). Mice were maintained on a normal chow diet (13.5% kcal fat; LabDiet) or high-fat diet (60% kcal fat; Research Diets) for 12 weeks to generate the diet induced obesity (DIO) model of glucose intolerance/insulin resistance. Of note, only male mice were used for all studies as female mice fail to develop glucose intolerance/insulin resistance following high-fat diet administration. Further, the DIO mouse model was used as the model of T2D due to its lack of genetic modifications to the leptin protein or receptor, which can impact immune cell function [50],[51]. The DIO mouse mirrors human physiology in dietary induced weight gain, development of insulin resistance and glucose intolerance [52]. Animals underwent all procedures at 20-24 weeks of age following confirmation of hyperglycemia. Body weights were determined prior to experimentation.

Fatty Acid Preparation

Sodium palmitate (P9767; Sigma-Aldrich) and lauric acid (w261416; Sigma-Aldrich) were prepared in accordance to previously established protocols [53]–[55] to limit LPS contamination by diluting a 50 mM stock solution in isopropanol into 10% fatty acid–free, low-endotoxin BSA (A-8806; Sigma-Aldrich; adjusted to pH 7.4) to obtain a 5 mM

palmitate-BSA stock solution that was filtered using a 0.22-mm low-protein binding filter (Millipore, Billerica, MA). Palmitate and laurate were added at 200 μM and 50 μM respectively, and BSA/ethanol was used in control treatments. The concentrations of palmitate and laurate were specifically chosen due to previous publication dosing recommendations as well as known FA plasma concentrations in T2D patients [21],[22],[53],[54].

Cell Culture and Cytokine Analysis

Bone marrow (BM) cells were collected by flushing mouse femurs and tibias with RPMI. BM-derived macrophages (BMDMs) were cultured as previously detailed [56]. On day 6, the cells were replated, and after resting for 24 h, they were stimulated with palmitate (200 μM; Sigma), laurate (50 μM; Sigma), BSA/ethanol, or LPS (100 ng/mL; Sigma (L2880) purified by phenol extraction <3% impurities) for 2-6 hours after which cells placed in Trizol (Invitrogen) for RNA analysis. For human monocyte-derived macrophages, CD14+ monocytes were cultures in complete media supplemented with 50ng/ml of M-CSF (R & D Systems) for 1 week. Adherent cells were washed and harvested with trypsin/EDTA (Lonza).

RNA Analysis

Total RNA extraction was performed using Trizol (Invitrogen) according to manufacturer's instructions. RNA was then reversed transcribed to cDNA using iScript (Biorad). PCR was performed with 2X Taqman PCR mix using the 7500 Real-Time PCR System. Primers for *Jmjd3* (Mm01332680_m1), *Il1b* (Mm00434228_m10), *Il12* (Mm01288992_m1), Human *JMJD3* (HS00389738_m1), Human *IL1β* (HS01555410_m1), and Human *Il12* (HS00233688_m1) were purchased (Applied Biosystems). 18S was used as the internal control. Data were then analyzed relative to 18s ribosomal RNA (2ΔCt). All samples were assayed in triplicate and expressed as a fold expression of the control sample. The threshold cycle values were used to plot a standard curve. Data were compiled in Microsoft Excel and presented using Prism software (GraphPad).

ChIP Assay

Chromatin immunoprecipitation (ChIP) assay was performed as described previously [56]. Briefly, cells underwent DNA-protein structure cross-linking by incubation in 1% formaldehyde for 10 minutes at 37°C. Following this, cells then were collected and lysed in 400 μL SDS lysis buffer. The resulting lysates were sonicated to obtain DNA fragments ranging from 200 to 1000 bp (base pairs) using a Branson Sonifier 450 (VWR, West Chester,

PA) under the following condition: 6 times for periods of 15 seconds each. After centrifuging, the supernatant containing chromatin was diluted, and an aliquot (2% volume) was saved to indicate the input DNA in each sample. The remaining chromatin fractions were precleared with salmon sperm DNA/protein A agarose beads followed by immunoprecipitation with the following antibodies: anti-H3K27trimethyl antibody (Abcam) or isotype control (rabbit polyclonal IgG) (Millipore) overnight at 4°C with gentle rotation. Cross-linking was reversed for 4 hours at 65°C and was followed by proteinase K digestion. DNA was purified by standard phenol/chloroform and ethanol precipitation and was subjected to real-time PCR.. Primers were designed using the Ensembl genome browser to search the IL1β, and IL12 promoter for NFκB within the promoter region and then NCBI Primer-BLAST was used to design primers that flank this site. Data are representative of 2-3 independent experiments. Primer sequences are available in Supplemental Table I.

Wound Digestion

Following sacrifice, wounds were collected from the backs of the mice postmortem following CO_2 asphyxiation using a 6 mm wound biopsy. Sharp scissors were used to excise the full thickness dermis with a 1-2mm margin around the wound ensuring collection of granulation tissue and wounds were placed in RPMI. Wounds were then carefully minced with sharp scissors and digested by incubating in a 50 mg/ml Liberase TM (Roche) and 20U/ml DNaseI (Sigma-Aldrich) solution. Wound cell suspensions were then gently plunged and filtered through a 100μm filter to yield a single cell suspension. Cells then underwent magnetic-activated cell sorted (MACs) and cultured ex-vivo[29].

Magnetic-Activated Cell Sorting (MACs) of Murine Wound and Human Monocyte Cell Isolates.

Wounds were digested as described above. Single cell suspensions were incubated with fluorescein isothiocyanate–labeled anti-CD3, anti-CD19, anti-NK1.1, and anti-Ly6G (BioLegend) followed by anti–fluorescein isothiocyanate microbeads (Miltenyi Biotec). Flow-through was then incubated with anti-CD11b microbeads (Miltenyi Biotec) to isolate the non-neutrophil, non-lymphocyte, CD11b+ cells. Cells were saved in Trizol (Invitrogen) for quantitative RT-PCR analyses. For human monocyte isolation, peripheral blood was collected and subjected to RBC lysis and Ficoll separation (GE healthcare). Cell suspensions were then treated with anti-human CD14 microbeads. Magnetic separation yielded 95% purity by flow cytometry.

ELISA/enzyme immunoassay

Murine wound macrophages were isolated as described above and cells were cultured at $2x10^5$ cells/well in a 24-well plate for 36 h in BSA, laurate (50 μM), palmitate (200 μM), or LPS. Supernatants were collected for enzyme immunoassay. Production of IL1β (R&D Systems DY401-05) and IL12 (R&D Systems M1270) was measured by enzyme immunoassay according to the manufacturer's instructions.

Wound Healing Assessment

Before wounding, mice were anesthetized, hair was removed with Veet (Reckitt Benckiser), and skin was cleaned with sterile water. Full-thickness back wounds were created by 4-mm punch biopsy as previously described [17]. Initial wound surface area was recorded and digital photographs were obtained daily using an Olympus digital camera. Photographs contained an internal scale to allow for standard measurement calibration. Wound area was quantified using ImageJ software (National Institutes of Health, Bethesda, MD) and was expressed as the percentage of original wound size over time. For Jmjd3 inhibitor injections, a stock solution of GSK-J4 (Tocris, Catalog 4594) of 5 mg/mL was prepared in dimethyl sulfoxide (DMSO) to

preserve stability. Before injection, the stock solution was diluted 1/10 with PBS (DMSO: PBS, 1:10 v/v). In systemic drug evaluation experiments, each mouse received daily i.p. injections (from 3 days prior to wounding until the entire wound has healed) of 400 μL of this solution equivalent to 10 mg/kg of the drug. Control mice received 400 μL of the vehicle during the same period.

Wound Histology

On day 3 post-wounding, whole wounds were excised using a 6mm punch biopsy. Wound sections were fixed in 10% formalin overnight before embedding in paraffin. 5 μm sections were stained with hematoxylin and eosin for evaluation of re-epithelialization and with Masson's Trichrome stain for collagen deposition. Images were captured using Olympus BX43 microscope and Olympus cell Sens Dimension software.

QUANTIFICATION AND STATISTICAL ANALYSIS

GraphPad Prism software (RRID:SCR_002798) version 6.0 was used to analyze the data. All the data were assessed for normality and equal variance using Shapiro-Wilk test and Levene test, respectively. Unpaired two-tailed Student's t test was used to determine statistical difference between two groups for normally distributed continuous variables. For comparison of multiple groups, one-way analysis of variance test followed by Newman-Keuls post hoc test. For data with small sample size or non-normally distributed data non-parametric Mann-Whitney test or Kruskal-Wallis test were used for analysis. All data are representative of at least two independent experiments as detailed in the figure legends. A P-value of less than or equal to 0.05 was significant.

Acknowledgements: We thank Robin Kunkel for her assistance with the graphical illustrations. This work is supported in part by National Institutes of Health grants R01-HL137919 (KG), F32-DK117545 (FD), Doris Duke Foundation (KG) American College of Surgeons Resident Fellowship (FD), and the Taubman Institute.

Author Contributions: KG, FD, SK, MO and AJ designed the experiments. FD, AD, AJ, SW, CA, and WM performed experiments. FD, AD, AJ, and SW analyzed data. FD, and KG prepared manuscript. FD and KG are the guarantors of this work and, as such, had full access to all the data in the study and takes responsibility for the integrity of the data and the accuracy of the data analysis.

Conflict of interest: The authors have no commercial or financial conflicts of interest

REFERENCES

1. **Smith KB**, **Smith MS**. Obesity Statistics. *Prim. Care - Clin. Off. Pract.* 2016; **43**:121–135.

2. **Kruidenier L, Chung C, Cheng Z, Liddle J, Che K, Joberty G, Bantscheff M, *et al.*** A selective jumonji H3K27 demethylase inhibitor modulates the proinflammatory macrophage response. *Nature*. 2012; **488**:404–8.

3. **Martinez FO**, **Helming L**, **Gordon S**. Alternative Activation of Macrophages: An Immunologic Functional Perspective. *Annu. Rev. Immunol.* 2009; **27**:451–483.

4. **Martinez FO**, **Sica A**, **Mantovani A**, **Locati M**. *Macrophage activation and polarization.* 2008.

5. **Lumeng CN**, **DeYoung SM**, **Bodzin JL**, **Saltiel AR**. Increased Inflammatory Properties of Adipose Tissue Macrophages Recruited During Diet-Induced Obesity. *Diabetes*. 2007; **56**:16–23.

6. **Wood S, Jayaraman V, Huelsmann EJ, Bonish B, Burgad D, Sivaramakrishnan G, Qin S, *et al.*** Pro-inflammatory chemokine CCL2 (MCP-1) promotes healing in diabetic wounds by restoring the macrophage response. Liu G, ed. *PLoS One*. 2014; **9**:e91574.

7. **Weisberg SP**, **McCann D**, **Desai M**, **Rosenbaum M**, **Leibel RL**, **Ferrante AW**. Obesity is associated with macrophage accumulation in adipose tissue. *J. Clin. Invest.* 2003; **112**:1796–808.

8. **Hewagama A**, **Richardson B**. The genetics and epigenetics of autoimmune diseases. *J. Autoimmun.* 2009; **33**:3–11.

9. **Jaenisch R**, **Bird A**. Epigenetic regulation of gene expression: how the genome integrates intrinsic and environmental signals. *Nat. Genet.* 2003; **33 Suppl**:245–54.

10. **Kimball AS, Joshi A, Carson WF, Boniakowski AE, Schaller M, Allen R, Bermick J, *et al.*** The Histone Methyltransferase MLL1 Directs Macrophage-Mediated Inflammation in Wound Healing and Is Altered in a Murine Model of Obesity and Type 2 Diabetes. *Diabetes*. 2017; **66**:2459–2471.

11. **Schlesinger Y, Straussman R, Keshet I, Farkash S, Hecht M, Zimmerman J, Eden E, *et al.*** Polycomb-mediated methylation on Lys27 of histone H3 pre-marks genes for de novo methylation in cancer. *Nat. Genet.* 2007; **39**:232–6.

12. **Lee JY**, **Sohn KH**, **Rhee SH**, **Hwang D**. Saturated Fatty Acids, but Not Unsaturated Fatty Acids, Induce the Expression of Cyclooxygenase-2 Mediated through Toll-like Receptor 4. *J. Biol. Chem.* 2001; **276**.

13. **Weigert C**, **Brodbeck K**, **Staiger H**, **Kausch C**, **Machicao F**, **Häring HU**, **Schleicher ED**. Palmitate, but not unsaturated fatty acids, induces the expression of interleukin-6 in human myotubes through proteasome-dependent activation of nuclear factor-kappaB. *J. Biol. Chem.* 2004; **279**:23942–52.

14. **Lancaster GI, Langley KG, Berglund NA, Kammoun HL, Reibe S, Estevez E, Weir J, *et al.*** Evidence that TLR4 Is Not a Receptor for Saturated Fatty Acids but Mediates Lipid-Induced Inflammation by Reprogramming Macrophage Metabolism. 2018; **27**:1096-1110.e5.

15. **Caesar R**, **Tremaroli V**, **Kovatcheva-Datchary P**, **Cani PD**, **Bäckhed F**. Crosstalk between Gut Microbiota and Dietary Lipids Aggravates WAT Inflammation through TLR Signaling. *Cell Metab.* 2015; **22**:658–68.

16. **Jia L, Vianna CR, Fukuda M, Berglund ED, Liu C, Tao C, Sun K, *et al.*** Hepatocyte Toll-like receptor 4 regulates obesity-induced inflammation and insulin resistance. *Nat. Commun.* 2014; **5**:3878.

17. **Gallagher KA, Joshi A, Carson WF, Schaller M, Allen R, Mukerjee S, Kittan N, *et al.*** Epigenetic changes in bone marrow progenitor cells influence the inflammatory phenotype and alter wound healing in type 2 diabetes. *Diabetes*. 2015; **64**:1420–30.

18. **Koh TJ**, **DiPietro LA**. Inflammation and wound healing: the role of the macrophage. *Expert Rev. Mol. Med.* 2011; **13**:e23.

19. **Na J, Lee K, Na W, Shin J-Y, Lee M-J, Yune TY, Lee HK, *et al.*** Histone H3K27 Demethylase JMJD3 in Cooperation with NF-κB Regulates Keratinocyte Wound Healing. *J. Invest. Dermatol.* 2016; **136**:847–858.

20. **Na J, Shin JY, Jeong H, Lee JY, Kim BJ, Kim WS, Yune TY, *et al.*** JMJD3 and NF-κB-dependent activation of Notch1 gene is required for keratinocyte migration during skin wound healing. *Sci. Rep.* 2017; **7**:6494.

21. **Clore JN**, **Allred J**, **White D**, **Li J**, **Stillman J**. The role of plasma fatty acid composition in endogenous glucose production in patients with type 2 diabetes mellitus. *Metabolism.* 2002; **51**:1471–7.

22. **Trombetta A**, **Togliatto G**, **Rosso A**, **Dentelli P**, **Olgasi C**, **Cotogni P**, **Brizzi MF**. Increase of palmitic acid concentration impairs endothelial progenitor cell and bone marrow-derived progenitor cell bioavailability: role of the STAT5/PPARγ transcriptional complex. *Diabetes*. 2013; **62**:1245–57.

23. **Yu S**, **Chen X**, **Xiu M**, **He F**, **Xing J**, **Min D**, **Guo F**. The regulation of Jmjd3 upon the expression of NF-κB downstream inflammatory genes in LPS activated vascular endothelial cells. *Biochem. Biophys. Res. Commun.* 2017; **485**:62–68.

24. **Welstead GG**, **Creyghton MP**, **Bilodeau S**, **Cheng AW**, **Markoulaki S**, **Young RA**, **Jaenisch R**. X-linked H3K27me3 demethylase Utx is required for embryonic development in a sex-specific manner. *Proc. Natl. Acad. Sci. U. S. A.* 2012; **109**:13004–13009.

25. **Chawla A**, **Nguyen KD**, **Goh YPS**. Macrophage-mediated inflammation in metabolic disease. *Nat. Rev. Immunol.* 2011; **11**:738–749.

26. **Ray I**, **Mahata SK**, **De RK**. Obesity: An Immunometabolic Perspective. *Front. Endocrinol. (Lausanne)*. 2016; **7**:157.

27. **Shi H**, **Kokoeva M V.**, **Inouye K**, **Tzameli I**, **Yin H**, **Flier JS**. TLR4 links innate immunity and fatty acid-induced insulin resistance. *J. Clin. Invest.* 2006; **116**:3015–3025.

28. **Falanga V**. Wound healing and its impairment in the diabetic foot. *Lancet (London, England)*. 2005; **366**:1736–43.

29. **Mirza RE**, **Fang MM**, **Ennis WJ**, **Koh TJ**. Blocking Interleukin-1 Induces a Healing-Associated Wound Macrophage Phenotype and Improves Healing in Type 2 Diabetes. *Diabetes*. 2013; **62**:2579–2587.

30. **Mirza RE**, **Fang MM**, **Weinheimer-Haus EM**, **Ennis WJ**, **Koh TJ**. Sustained inflammasome activity in macrophages impairs wound healing in type 2 diabetic humans and mice. *Diabetes*. 2014; **63**:1103–14.

31. **Mirza RE**, **Fang MM**, **Novak ML**, **Urao N**, **Sui A**, **Ennis WJ**, **Koh TJ**. Macrophage PPARγ and impaired wound healing in type 2 diabetes. *J. Pathol.* 2015; **236**:433–44.

32. **Huang S, Rutkowsky JM, Snodgrass RG, Ono-Moore KD, Schneider DA, Newman JW, Adams SH, *et al.*** Saturated fatty acids activate TLR-mediated proinflammatory signaling pathways. *J. Lipid Res.* 2012; **53**:2002–13.

33. **Nagareddy PR, Kraakman M, Masters SL, Stirzaker RA, Gorman DJ, Grant RW, Dragoljevic D, *et al.*** Adipose tissue macrophages promote myelopoiesis and monocytosis in obesity. *Cell Metab.* 2014; **19**:821–35.

34. **Osborn O**, **Olefsky JM**. The cellular and signaling networks linOsborn, O., & Olefsky, J. M. (2012). The cellular and signaling networks linking the immune system and metabolism in disease. Nature Medicine, 18(3), 363–74. doi:10.1038/nm.2627king the immune system and metabolism i. *Nat. Med.* 2012; **18**:363–74.

35. **Davis FM, denDekker A, Kimball A, Joshi AD, El Azzouny M, Wolf SJ, Obi AT, *et al.*** Epigenetic Regulation of TLR4 in Diabetic Macrophages Modulates Immunometabolism and Wound Repair. *J. Immunol.* 2020; **204**:2503–2513.

36. **Edwards TM**, **Myers JP**. Environmental exposures and gene regulation in disease etiology. *Environ. Health Perspect.* 2007; **115**:1264–70.

37. **Skinner MK**, **Manikkam M**, **Guerrero-Bosagna C**. Epigenetic transgenerational actions of environmental factors in disease etiology. *Trends Endocrinol. Metab.* 2010; **21**:214–22.

38. **Kumar S**, **Pamulapati H**, **Tikoo K**. Fatty acid induced metabolic memory involves alterations in renal histone H3K36me2 and H3K27me3. 2016; **422**:233–242.

39. **Zhong Q**, **Kowluru RA**. Role of histone acetylation in the development of diabetic retinopathy and the metabolic memory phenomenon. *J. Cell. Biochem.* 2010; **110**:1306–13.

40. **Togliatto G**, **Dentelli P**, **Brizzi MF**. Skewed Epigenetics: An Alternative Therapeutic Option for Diabetes Complications. *J. Diabetes Res.* 2015; **2015**:373708.

41. **Wegner M**, **Neddermann D**, **Piorunska-Stolzmann M**, **Jagodzinski PP**. Role of epigenetic mechanisms in the development of chronic complications of diabetes. *Diabetes Res. Clin. Pract.* 2014; **105**:164–75.

42. **Davis FMFMFMFM**, **Kimball A**, **Boniakowski A**, **Gallagher K**. Dysfunctional Wound Healing in Diabetic Foot Ulcers: New Crossroads. *Curr. Diab. Rep.* 2018; **18**:2.

43. **Lochmann TL, Powell KM, Ham J, Floros K V, Heisey DAR, Kurupi RIJ, Calbert ML, *et al.*** Targeted inhibition of histone H3K27 demethylation is effective in high-risk neuroblastoma. *Sci. Transl. Med.* 2018; **10**.

44. **Taylor KR**, **Trowbridge JM**, **Rudisill JA**, **Termeer CC**, **Simon JC**, **Gallo RL**. Hyaluronan Fragments Stimulate Endothelial Recognition of Injury through TLR4. *J. Biol. Chem.* 2004; **279**:17079–17084.

45. **Asea A, Rehli M, Kabingu E, Boch JA, Baré O, Auron PE, Stevenson MA, *et al.*** Novel signal transduction pathway utilized by extracellular HSP70. Role of toll-like receptor (TLR) 2 and TLR4. *J. Biol. Chem.* 2002; **277**:15028–15034.

46. **Wang X**, **Cao Q**, **Yu L**, **Shi H**, **Xue B**, **Shi H**. Epigenetic regulation of macrophage polarization and inflammation by DNA methylation in obesity. *JCI insight*. 2016; **1**:e87748.

47. **El-Osta A, Brasacchio D, Yao D, Pocai A, Jones PL, Roeder RG, Cooper ME, *et al.*** Transient high glucose causes persistent epigenetic changes and altered gene expression during subsequent normoglycemia. *J. Exp. Med.* 2008; **205**:2409–2417.

48. **Parathath S**, **Grauer L**, **Huang L-S**, **Sanson M**, **Distel E**, **Goldberg IJ**, **Fisher EA**. Diabetes adversely affects macrophages during atherosclerotic plaque regression in mice. *Diabetes*. 2011; **60**:1759–69.

49. **Reddy MA**, **Zhang E**, **Natarajan R**. Epigenetic mechanisms in diabetic complications and metabolic memory. *Diabetologia*. 2015; **58**:443–55.

50. **Mancuso G, Midiri A, Beninati C, Piraino G, Valenti A, Nicocia G, Teti D, *et al.*** Mitogen-activated protein kinases and NF-kappa B are involved in TNF-alpha responses to group B streptococci. *J. Immunol.* 2002; **169**:1401–9.

51. **Loffreda S, Yang SQ, Lin HZ, Karp CL, Brengman ML, Wang DJ, Klein AS, *et al.*** Leptin regulates proinflammatory immune responses. *FASEB J.* 1998; **12**:57–65.

52. **Parekh PI**, **Petro AE**, **Tiller JM**, **Feinglos MN**, **Surwit RS**. Reversal of diet-induced obesity and diabetes in C57BL/6J mice. *Metabolism.* 1998; **47**:1089–96.

53. **Riera-Borrull M**, **Cuevas VD**, **Alonso B**, **Vega MA**, **Joven J**, **Izquierdo E**, **Corbí ÁL**. Palmitate Conditions Macrophages for Enhanced Responses toward Inflammatory Stimuli via JNK Activation. *J. Immunol.* 2017; **199**:3858–3869.

54. **Wang Y, Qian Y, Fang Q, Zhong P, Li W, Wang L, Fu W, *et al.*** Saturated palmitic acid induces myocardial inflammatory injuries through direct binding to TLR4 accessory protein MD2. *Nat. Commun.* 2017; **8**:13997.

55. **Ahmad R, Al-Roub A, Kochumon S, Akther N, Thomas R, Kumari M, Koshy MS, *et al.*** The Synergy between Palmitate and TNF-α for CCL2 Production Is Dependent on the TRIF/IRF3 Pathway: Implications for Metabolic Inflammation. *J. Immunol.* 2018; **200**:3599–3611.

56. **Ishii M, Wen H, Corsa CAS, Liu T, Coelho AL, Allen RM, Carson WF, *et al.*** Epigenetic regulation of the alternatively activated macrophage phenotype. *Blood*. 2009; **114**:3244–54..

FIGURE LEGENDS

Figure 1. Palmitate induces Jmjd3 and proinflammatory phenotype in bone marrow derived macrophages via the TLR4 pathway. A, B. Bone marrow derived macrophages (BMDMs) harvested from control C57BL/6 mice were stimulated with BSA, palmitate (200 μM), Laurate (50 μM), or LPS for 6 hours after which they were collected for analysis. *Jmjd3*, *Il1b*, and *Il12* expression was quantified by qPCR and normalized to BSA treatment. *p< 0.05, **p< 0.01 by ANOVA followed by Newman–Keuls post hoc test. (n =5 mice per group, data shown above is of a single representative experiment with experiment repeated two times with three technical replicates in each experiment). **B.** ChIP analysis for H3K27me3 at the NF-kB binding site of the *IL1b* or *Il12* promoter in control BMDMs following stimulation with BSA, palmitate (200 μM), or Laurate (50 μM). (n =5 mice per group, data shown above is of a single representative experiment with experiment repeated two times with three technical replicates in each experiment). *p<0.05 by ANOVA followed by Newman–Keuls post hoc. **C.** BMDMs were harvested from control C57BL/6, $TLR4^{-/-}$ or $MyD88^{-/-}$ mice and then stimulated with BSA, palmitate (200 μM), or Laurate (50 μM) for 6 hours after which they were collected for analysis. *Jmjd3*, *Il1b*, and *Il12* expression was quantified by qPCR and normalized to BSA treatment. For ChIP experiments, isotype control antibody to IgG was run in parallel. Dotted line represents isotype control. (n =5 mice per group, data shown above is of a single representative experiment with experiment repeated two times with three technical replicates in each experiment). **p< 0.01 by ANOVA followed by Newman–Keuls post hoc test. Data are presented as the mean±SEM.

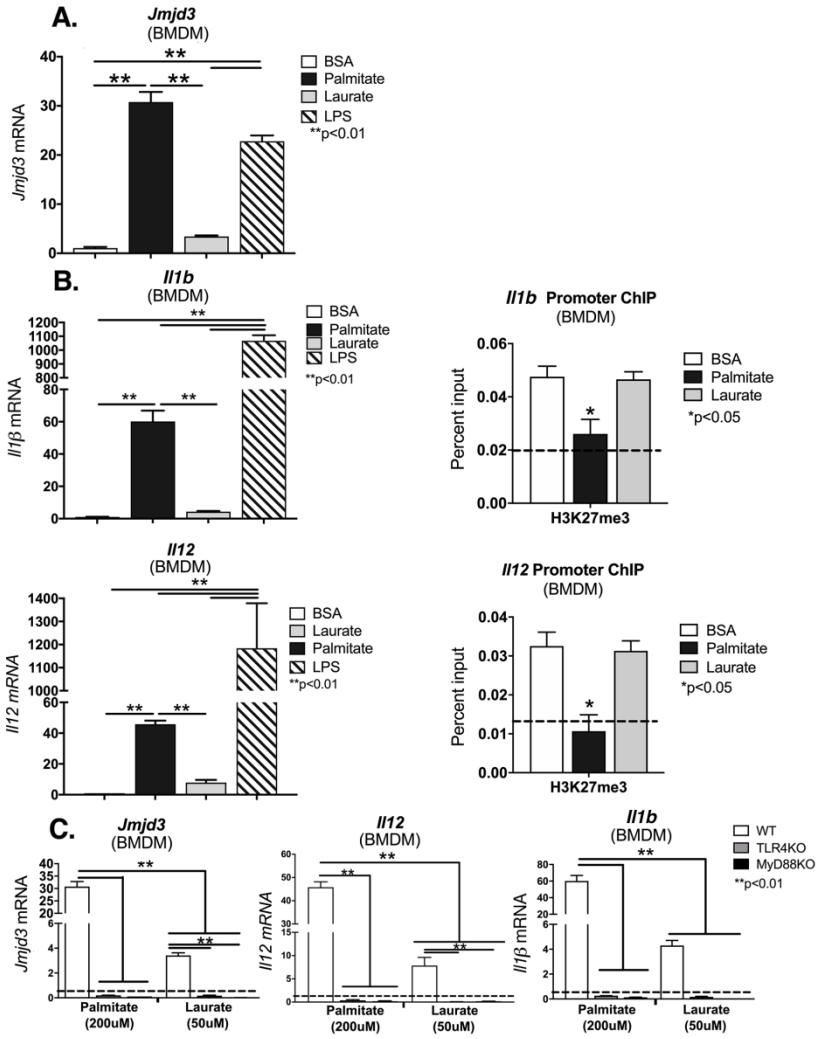

Figure 2. Palmitate induces Jmjd3 and proinflammatory phenotype in *in vivo* wound macrophages. A. Wound macrophages [CD11b^{+}(CD3^{-}, CD19^{-}, NK1.1^{-}, Ly6G^{-})] were MACS isolated from control C57BL/6 on post-injury day 3 and stimulated with BSA, palmitate (200 μM), or Laurate (50 μM) for 24 hours. *Jmjd3* expression was quantified by qPCR and normalized to BSA treatment (n =3 mice per group, data shown above is of a single representative experiment with experiment repeated two times with three technical replicates in each experiment). *p< 0.05 by ANOVA followed by Newman–Keuls post hoc test. **B, C.** Wound macrophages [CD11b^{+}(CD3^{-}, CD19^{-}, NK1.1^{-}, Ly6G^{-})] were MACs isolated from control C57BL/6 on post-injury day 3 and stimulated with BSA, palmitate (200 μM), or Laurate (50 μM) for 24 hours. *Il1b* and *Il12* expression was quantified by qPCR and expressed as fold comparison to BSA treatment. ChIP analysis for H3K27me3 was performed on wound macrophages at the NF-kB binding site of the *Il1b* and *Il12* promoter (n =5 mice per group, data shown above is of a single representative experiment with experiment repeated two times with three technical replicates in each experiment). **p<0.01 by ANOVA followed by Newman–Keuls post hoc. **D, E.** Wound macrophages

($CD11b^+[CD3^-CD19^-NK1.1^-Ly6G^-]$) on day 3 via MACs sorting and stimulated the macrophages with palmitate with or without co-administration of a Jmjd3 specific inhibitor (GSK-J4, 5μM). *Il1b* and *Il12* gene expression was measured by qPCR and normalized to 18S. (n =5 mice per group, data shown above is of a single representative experiment with experiment repeated two times with three technical replicates in each experiment). **p<0.01 by ANOVA followed by Newman–Keuls post hoc. Data are presented as the mean±SEM.

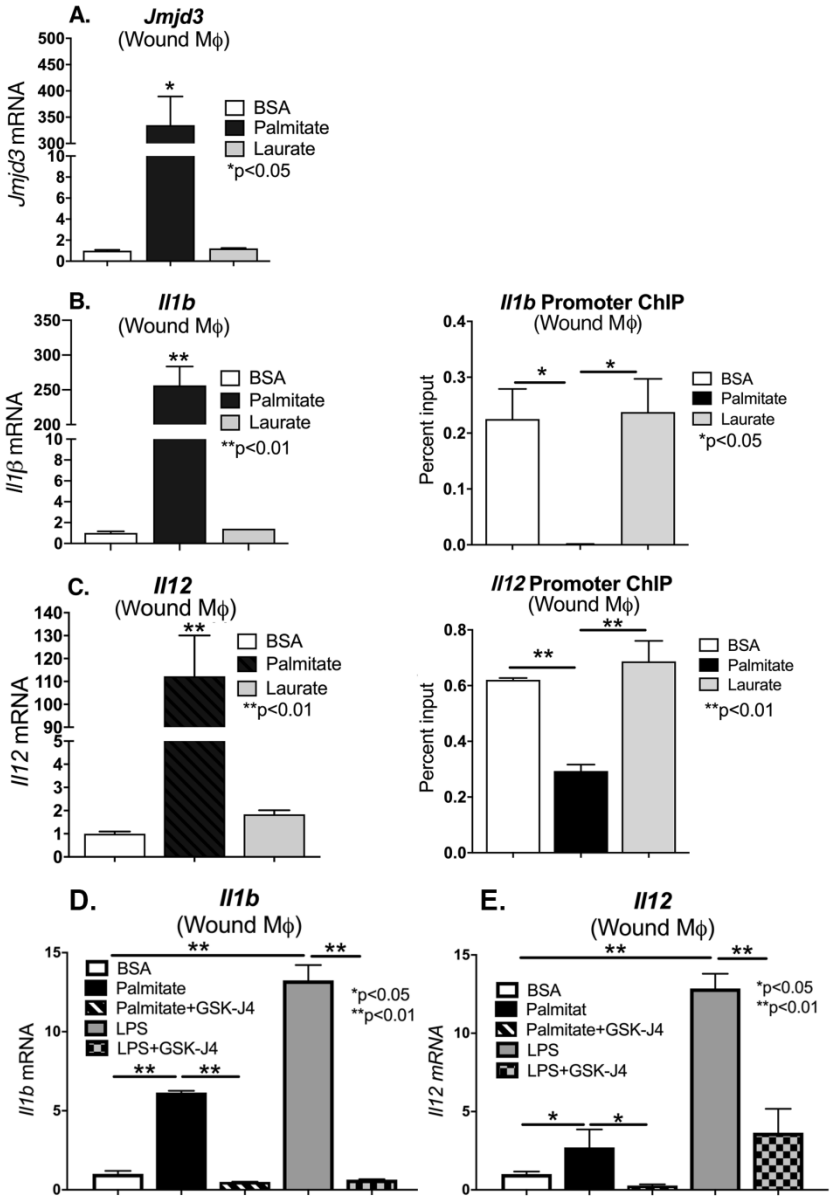

Figure 3. Palmitate stimulates *JMJD3* and proinflammatory cytokine expression in human monocytes. A-B. Peripheral blood (30 mL) was collected from patients without diabetes. Peripheral blood mononuclear cells underwent Ficoll separation. $CD14^+$ monocytes were then positively selected by MACS and underwent ex vivo stimulation with BSA, palmitate (200 μM), or Laurate (50 μM) for 8 hrs. *JMJD3, IL1b,* and *TNFa* gene expression was measured by qPCR and normalized to 18S. (n =3 patients per group, data shown above is of a single representative experiment with experiment repeated two times with three technical replicates in each experiment). **p<0.01 by ANOVA followed by Newman–Keuls post hoc. Data are presented as the mean±SEM.

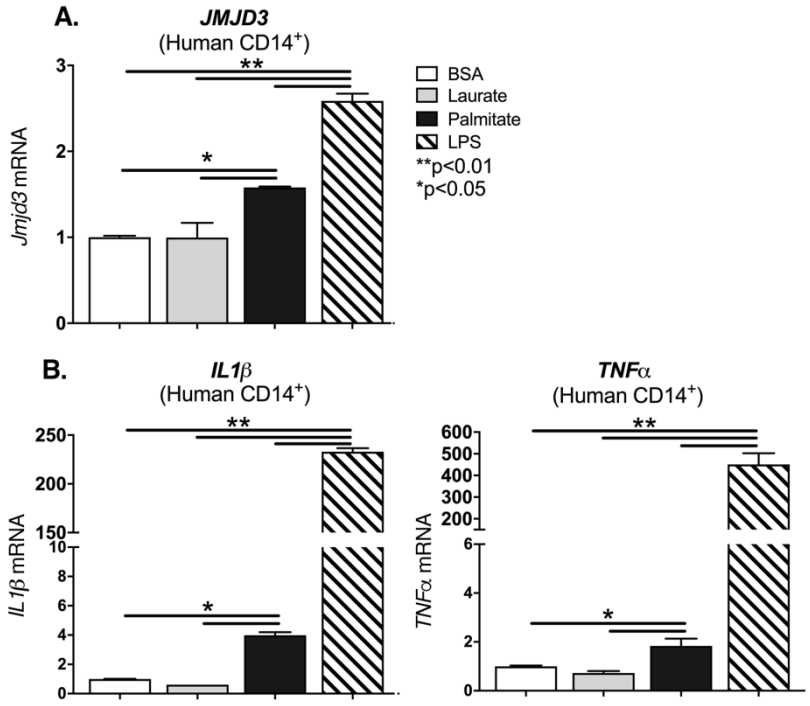

Figure 4. Pharmacological inhibition of JMJD3 improves early diabetic wound healing. A. Wounds were created in DIO mice and treated with daily injections of GSK-J4 (10 mg/kg) or PBS control starting 3 days prior to wounding and daily following wounding. Wound size was measured by blinded observed in Image J NIH. Representative photographs of the wounds of DIO mice with PBS injection and DIO mice with GSK-J4 injection on days 0 and 3 post injury are shown (n =5 mice per treatment group, data shown above is of a single representative experiment with experiment repeated two times with 5 mice per treatment group in each experiment). **B, C.** Circulating monocytes and wound macrophages were MACS isolated from DIO mice + PBS injection and DIO mice + GSK-J4 injection on day 3 following injury. *Il1b*, *Tnf*, *Il12,* and *Nos* expression was quantified by qPCR and each gene expressed as fold comparison to DIO + PBS level. (n =3 mice per group, data shown above is of a single representative experiment with experiment repeated two times with three technical

replicates in each experiment). *p<0.05 by Mann-Whitney U test. Data are presented as the mean±SEM.

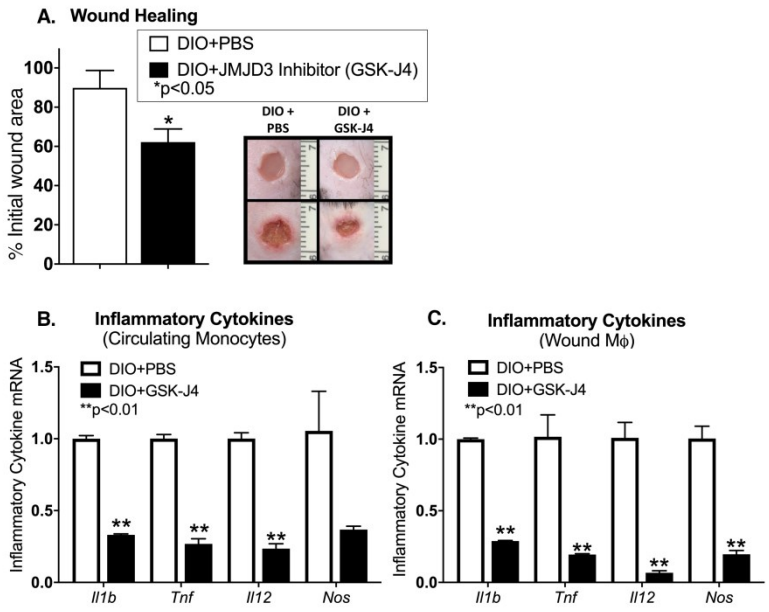

Figure 5. Palmitate Regulates Jmjd3 Epigenetic Modifications in Diabetic Wound Macrophages. Schematic demonstrates the role of palmitate regulation of JMJD3 in macrophages in both normal and diabetic wound healing.

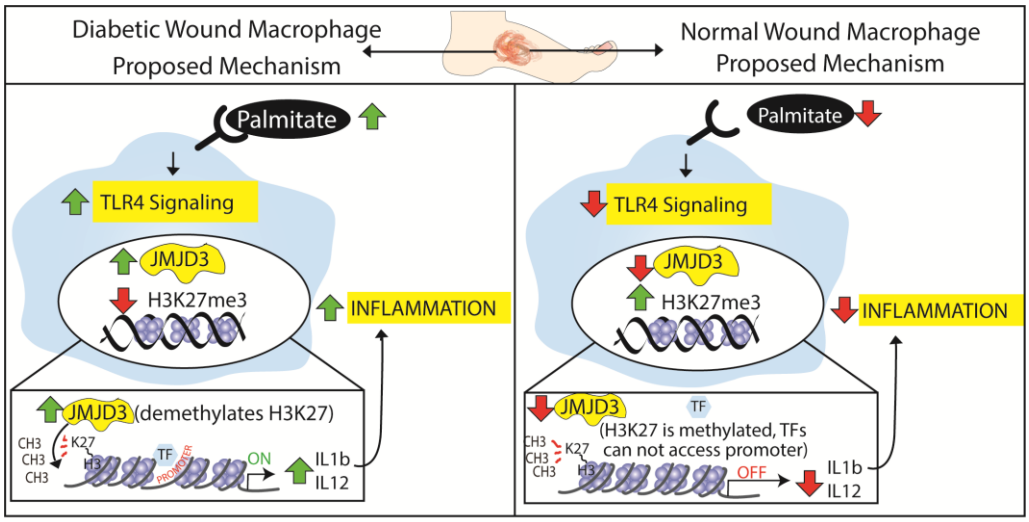

Graphic Abstract Text

Palmitate drives chronic macrophage mediated inflammation in diabetic tissue via upregulation of the histone demethylase, Jmjd3, and a histone demethylase inhibitor-based therapy may represent a novel treatment for non-healing diabetic wounds.